

Dry Sliding Tribological Studies on Zinc-Aluminium Alloys with varying Aluminium Contents using Pin-on-Disc Tribometer

Anand Mani*, V.V. Manikandan, P.K. Rajendrakumar

Department of Mechanical Engineering, National Institute of Technology, Calicut, Kerala-673601, India

*Corresponding author email: mani.aanand@gmail.com, Tel.: +91 9450461618

ABSTRACT

Zn-based alloys with different Al-content was prepared using Conventional melting and casting approach. Rockwell and Vickers's hardness tests were performed in which hardness increased with increase in Al-content. SEM-EDS analysis of ZA8.19 alloys showed coarse η -Zn rich dendrite and $\alpha+\eta$ eutectoid colonies, ZA10.5 revealed finer η -Zn rich dendrites but more $\alpha+\eta$ eutectoid than ZA8.19 while ZA19.43 revealed α -Al rich dendrites surrounded by $\alpha+\eta$ eutectoid. Pin-on-Disc Tribometer at a speed of 0.5 m/s and 2 m/s was used to test sliding distance over a load range of 10 N and 70 N upto trial distance of 1000 m and observed that steady-state wear was reached before 1000 m of sliding in all three cases and thus was fixed for all tests. Load test was conducted over wide range of 10 N, 30 N, 50 N, and 70 N with 0.5 m/s as sliding speed and found that as Al-content increased in Zinc alloys, the weight loss increased with the increase in load with some exceptional cases. In sliding speed test, conducted over a range of 0.5 m/s, 1 m/s, 1.5 m/s and 2 m/s with load 70 N, results showed that as the Al-content increased, the weight loss decreased with increase in sliding speed with exceptional case. Overall, ZA19.43 was found to be the most wear resistant material among the three.

Keywords – Zinc-based alloys, Hardness, SEM-EDS analysis, Tribometer; Weight loss.

1. INTRODUCTION

Due to the high cost of present bearing materials, the automotive and machine tool sectors are in immediate need of materials having improved tribological properties with low material cost compared to conventional bearing materials [1]. During World War II, Germany faced critical copper shortage that forced the consideration of alternative materials for bronze. Most of the zinc alloys developed during that period was used throughout the war. However, those containing 8 to 28% of aluminium have drawn attention in view of the attainment of good mechanical and tribological properties [2].

The advantages of using such zinc alloy bearings is that it has low cost, low density, better stability, long running life, high load bearing capability and better dry running characteristics. These alloys were developed to be used for the condition of limiting lubrication. They can be used successfully as bearing materials, especially for high load and low-speed condition. The other benefits of such alloys are pollution-free handling and better energy saving in casting and melting [2]. In 1962, the International Lead Zinc Research Organization (ILZRO) introduced ILZRO 12 (as ZA-12) [3]. In the late 1970s, the Noranda Research Centre developed two additional

alloys, ZA-8 and ZA-27. These alloys were developed to compete with other mature alloy systems, such as brass, bronze, aluminium-based alloys and cast iron.

Aluminium acts as an essential alloying elements in Zn-based alloys which provide fluidity to the alloys [3, 4]. Based on practical aspect, the quantity of Aluminium added to Zn alloys in the hope to achieve good mechanical properties varies widely. It was found that wear resistance was obtained by increasing Al-weight percentage [4]. An addition of magnesium and copper in small quantity to Zn-based alloys helps in achieving good castability and mechanical properties [5]. Since the new member of zinc alloys which were developed such as ZA8, ZA12 and ZA27 contains less than 3 wt. % of copper.

In present work, tribological studies have been done to compare three different zinc-based alloys i.e. ZA8.19, ZA10.5 and ZA19.43 with varying aluminium contents using Pin-on-Disc Tribometer by varying the parameters such as load and sliding speed. But in these alloys, copper content is more than 3 wt. %. In this paper, along with wear test, resulting microstructural features and hardness of the Zinc-Aluminium alloys have also been discussed.

2. EXPERIMENTAL WORK

2.1 Preparation of the alloy specimens

To determine the most suitable chemical composition, three zinc-based alloys i.e. ZA8.19, ZA10.5, and ZA19.43 were prepared by permanent mould casting. Firstly, the respective amount of material were extracted by percentage weight required to make such alloys. The melting of material was done at 480 °C. A small 100 kg furnace was used, and the melting was done manually in a crucible. Then materials were transferred to a permanent mould into a diameter specially made for order. As-cast zinc-based alloys were found to have casting defects and irregular surface finish. So all three zinc-based alloys have been turned with lathe machine to give smooth surface finish. Each of these alloys was then cut into four parts along the length and were turned to lathe machine to get 8 mm diameter rod. The pins were made to 8 mm diameter and 30 mm length and were used for friction and wear tests using the pin-on-disc tribometer.

2.2. Composition

The composition test was conducted for ZA8.19, ZA10.5 and ZA19.43 alloys using SEM-EDS. For all the three zinc-based alloys, Zinc acts as primary material (99.97% pure) and aluminium as secondary material (99.96% pure). To have reasonable mechanical properties and castability, some amount of copper is also added to this alloy.

2.3. Hardness

Hardness test was conducted using Rockwell hardness and Vickers hardness test machine. Rockwell hardness test uses steel ball as indenter under the load 10 kgf and application time of load was 60 seconds. Vickers hardness test comprises of the diamond indenter. The load applied during measurement was 10 kgf and dwell time used was 10 seconds.

2.4. Metallography

Metallography test was conducted to find out the microstructure of all three specimens. Specimens were ground with emery paper and then the polishing was done on rotating wheels covered by a velvet cloth with diamond paste [6]. The pad should be kept well supplied with diamond polishing pump spray [7]. The specimen was etched with an etchant nital having the composition of 100 ml alcohol and 0.5-5 ml HNO₃. Immersion time for etchant was 20 seconds with 5% nital and rest water

[8]. Specimens were then examined using scanning electron microscope (SEM).

2.5. Friction and wear test

Friction and wear test was conducted using pin-on-disc tribometer by varying load and sliding speed. The pin used had a dimension of 8 mm diameter and 30 mm length. The disc used was steel of hardness 60 HRC. A test was conducted to fix sliding distance. In sliding distance test, low and high load i.e. 10 N and 70 N and low and high sliding speed i.e. 0.5 m/s and 2 m/s was selected. Wear track diameter is fixed as 100 mm and sliding distance as 1000 m. The aim of such test is to obtain steady-state wear rate before 1000 m sliding. If in all cases, steady-state wear appears before 1000 m sliding, we will fix 1000 m as the sliding distance for all the tests to be performed in future. Load variation test was conducted by varying load as 10 N, 30 N, 50 N and 70 N and keeping sliding speed 0.5 m/s and sliding distance 1000 m as fixed parameters. Sliding speed variation test was conducted by varying sliding speed as 0.5 m/s, 1 m/s, 1.5 m/s and 2 m/s and keeping load 70 N and sliding distance 1000 m as fixed parameters. Each test is conducted thrice, and their average value has been plotted.

3. RESULTS AND DISCUSSIONS

3.1. Composition and hardness test

The composition of all three Zinc-based alloys has been well tested and found that ZA8.19 consisted of 8.19% of Al and 11.78% of Cu. ZA10.5 consisted of 10.5% of Al and 9.36% of Cu whereas ZA19.43 consisted of 19.43% of Al and 7.14% of Cu. All these zinc-based alloys contained balanced weight % of zinc which has been well described in Table 1.

Table 1: Composition of all three Zinc-based alloys

Specimens	Al (Wt. %)	Cu (Wt. %)	Zn (Wt. %)
ZA 8.19	8.19	11.78	Balance
ZA 10.5	10.5	9.36	Balance
ZA 19.43	19.43	7.14	Balance

The hardness test of these alloys has been tested and measured through two well established parameters such as Rockwell hardness test and Vickers hardness test as described in Table 2. In Rockwell hardness test, it was observed that as aluminium content increased in zinc-based alloys, the hardness of the material increased. In order to verify if the sequence of hardness value

obtained using Rockwell hardness test machine is correct or false, another hardness test was conducted using Vickers's hardness test machine and the sequence obtained were similar to the Rockwell hardness tester which verified it.

Table 2: Hardness measurement of Zinc alloys using various parameters

Zinc alloys	Rockwell hardness tester	Vickers's hardness tester
ZA 8.19	88	115.36
ZA 10.5	88.33	116.23
ZA 19.43	93.16	122.16

3.2. Metallography

The microstructure of ZA8.19 consists of coarse η -Zn rich dendrite and $\alpha+\eta$ eutectoid colonies as shown in Fig 1(a) [5]. α - Al fcc phase is also present but is less as compared to zinc. In SEM image, the white coloured dot represents copper compounded zinc i.e. $CuZn_4$. It is observed that grains are loosely packed. Hence, it is a softer material. The microstructure of ZA10.5 contains finer η -Zn rich dendrite and more $\alpha+\eta$ eutectoid colonies than that of ZA8.19 as shown in Fig. 1(b) [5]. In this too copper compounded zinc can be observed. This material is slightly harder than ZA8.19 as grain arrangement is better. The microstructure of ZA19.43 consists of α -Al rich dendrites and surrounded by $\alpha+\eta$ eutectoid as shown in Fig. 1(c) [5]. It is observed that grains are closely packed, and hence it is harder than ZA8.19 and ZA10.5. Blowholes can also be seen due to casting defects.

3.3. Friction and wear test

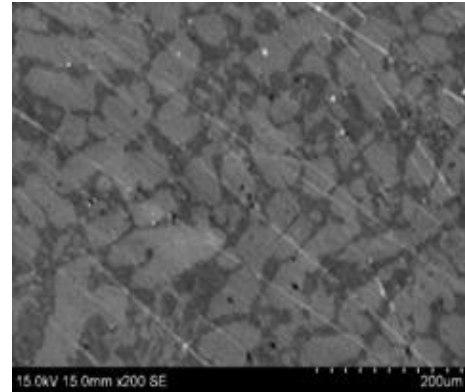
3.3.1. Test to fix sliding distance

Test to fix sliding distance were carried out on Pin-on-Disc Tribometer at a speed of 0.5 m/s and 2 m/s over a load range of 10 N and 70 N at a sliding distance 1000 m for all three specimens. It was observed that for all cases, the steady-state wear was reached before 1000 m of sliding. Hence, fixing 1000 m as the sliding distance is justified.

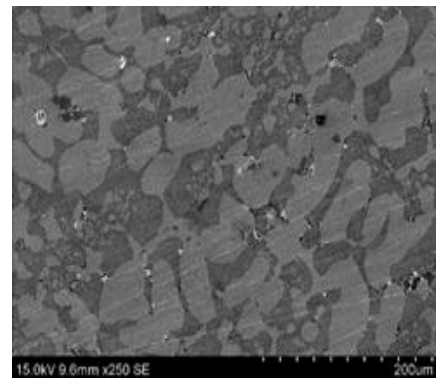
3.3.2. Load variation test

The load test is carried out by varying load as 10 N, 30 N, 50 N and 70 N and keeping sliding speed as 0.5 m/s and sliding distance as 1000 m constant. The graph between weight loss vs. specimens and frictional coefficient vs. specimens has been plotted. Before performing wear test, each specimen pin is polished with the emery paper of

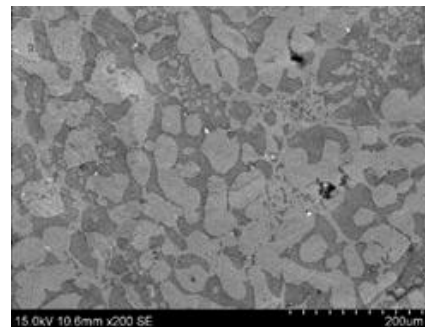
grit size 100, 220, 320, 400, 600, 1000, 1500, 2000 and 3000. The pin is then washed with acetone and then its weight is measured in weighing balance. The test was conducted, and the weight of the pin was measured once again after the test. This way weight loss of the pin was obtained. The frictional coefficient was obtained from the software itself and then the results were plotted.



(a)



(b)



(c)

Fig. 1: Microstructures of (a) ZA8.19, (b) ZA10.5 and (c) ZA19.43

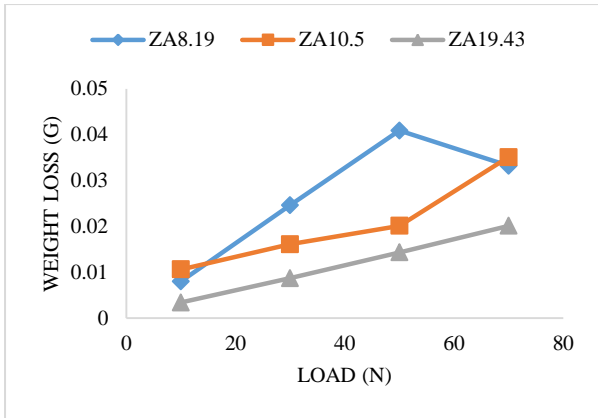


Fig. 2: Weight loss as a function of load for ZA8.19, ZA10.5 and ZA19.43

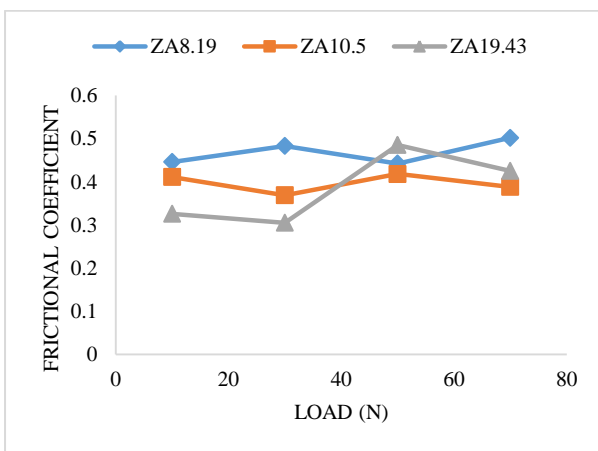
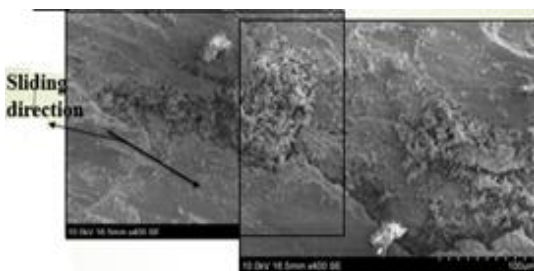
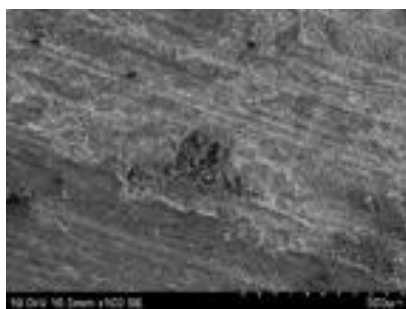


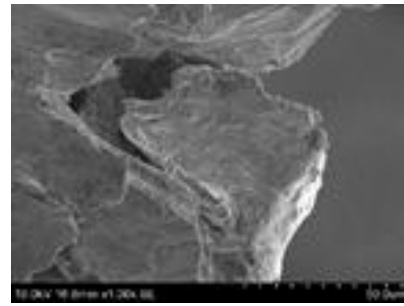
Fig. 3: Frictional coefficient as a function of load for ZA8.19, ZA10.5 and ZA19.43



(a)



(b)



(c)

Fig. 4: Scanning Electron Microscope (SEM) image of ZA8.19 at load 50 N and Sliding speed 0.5 m/s (a) shows a very rough surface due to more plastic deformation and strain rate (b) shows grooves and scratch marks and (c) shows the removal of material from the edge of the pin due to the crack propagation through the grain boundaries.



(a)



(b)

Fig. 5: Scanning Electron Microscope (SEM) image of ZA8.19 at load 70 N and Sliding speed 0.5 m/s. (a) shows occurrence of delamination and (b) shows thin grooves due to abrasion

Fig. 2 showed the graphical representation of variation of weight loss with load. The result shows that the weight loss of all the three specimens increases with

increase in load (except for the case in which weight loss of ZA8.19 decreases when the load is increased beyond 50 N) whereas figure 3 showed the graphical representation of approximately constant value of frictional coefficient for ZA8.19 and ZA10.5, but for ZA19.43, it is seen that when the load is increased from 30 N to 50 N, frictional coefficient increases with the increase in weight loss. The Scanning Electron Microscope (SEM) image of ZA8.19 at load 50 N and 70 N with Sliding speed 0.5 m/s has been shown in Fig. 4 and Fig. 5, respectively.

It is found that the weight loss is increased with the increase in load due to increase in frictional force. With the increase in frictional force, the surface temperature is increased. Initially, there was a contact between sharp asperities. When the load is increased, the stress concentrates on the sharp asperities area, which in turn leads to soft distortion of this asperities. Since the asperities contains hard particle like CuZn₄ as studied in microstructure test, these hard asperities rolls down between the contacts due to plastic deformation, which results in development of crack at the sub surface. The crack nucleates and merge together due to the stress propagation during sliding and joins the wear surface; the detachment of the material takes place. Hence, delamination occurs which can be seen in fig 5 (a) and Fig 5 (b) that shows thin grooves formed due to abrasion. The only difference why the ZA8.19 showed higher weight loss at a lower load of 50 N (compared to 70 N) is due to the removal of material from the edge of the pin.

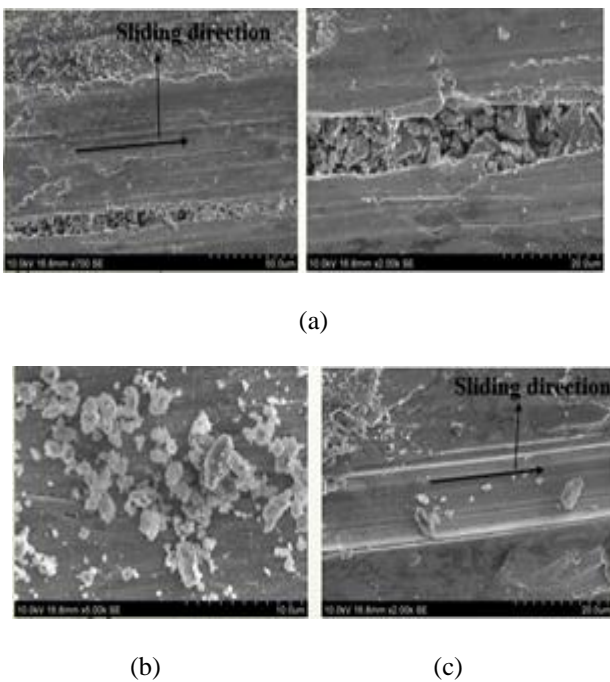


Fig. 6: Scanning Electron Microscope (SEM) image of

ZA10.5 at load 70 N and Sliding speed 0.5 m/s. (a) shows that delamination process has occurred with observance of some flakes (b) shows loose wear particles which are back transferred to the surface during sliding whereas (c) shows grooves due to abrasion

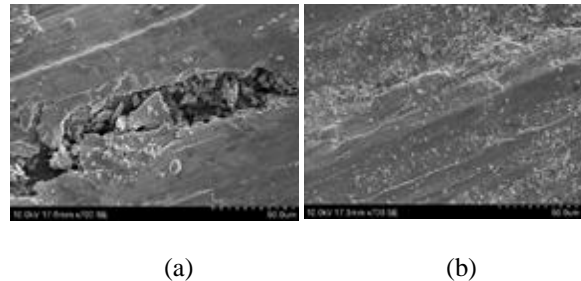


Fig. 7: Scanning Electron Microscope (SEM) image of ZA19.43 at load 70 N and Sliding speed 0.5 m/s (a) shows rough surface due to plastic deformation and (b) shows some flakes and grooves.

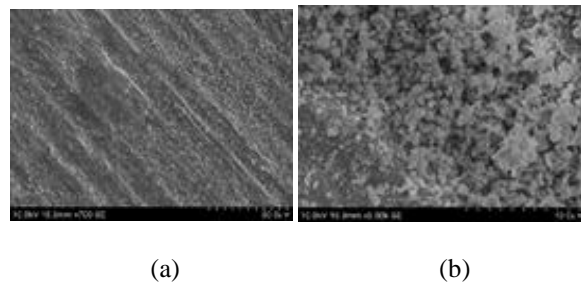


Fig. 8: Scanning Electron Microscope (SEM) image of ZA19.43 at load 10 N and Sliding speed 0.5 m/s. (a) shows smoother surface and (b) shows loose wear particle back transferred on the surface during sliding

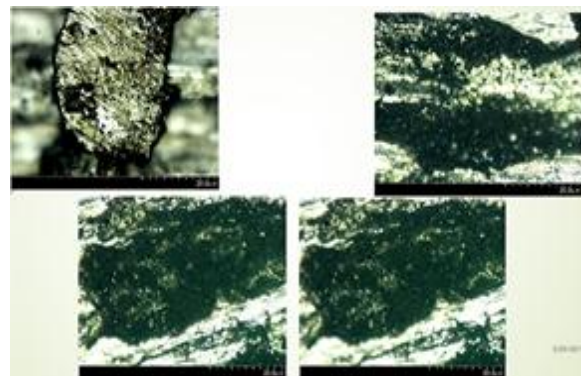


Fig. 9: Microstructure of pin surface after the test showing wear debris adhere to the pin surface

Further, the SEM image of ZA10.5 at load 70 N and sliding speed 0.5 m/s in Fig. 6 (a) showed that delamination process has occurred with observance of some flakes. Fig. 6 (b) shows loose wear particles

which are back transferred to the surface during sliding whereas Fig. 6 (c) shows grooves due to abrasion. The SEM image of ZA19.43 at load 70 N and Sliding speed 0.5 m/s in Fig. 7 (a) shows rough surface due to plastic deformation whereas Fig. 7 (b) shows some flakes and grooves.

Since Fig. 6 (a) shows large removal of material from the surface due to delamination process. Hence, the weight loss of ZA10.5 at load 70 N and sliding speed 0.5 m/s is observed to be higher. ZA19.43 showed smoother surface when tested at load 10 N and sliding speed 0.5 m/s with a loose wear particle back transferred on the surface during the sliding as seen in Fig. 8 (a) and Fig. 8 (b). On the other hand, ZA19.43 at load 70 N and sliding speed 0.5 m/s showed very rough surface and some flakes and grooves due to abrasion as seen in Fig. 7 (a) and Fig. 7 (b). Hence, the weight loss of ZA19.43 is increased with the increase in load as shown in Fig. 2. Fig. 9 showed the loose wear debris which got back transferred due to repeated unidirectional sliding. The variation of load test concludes that ZA19.43 performs much better than ZA8.19 and ZA10.5 in tribological test. Hence, ZA19.43 is more wear resistant material among the three.

3.3.3 Sliding speed variation test

Sliding speed variation test is conducted on Pin-on-Disc Tribometer by varying sliding speed as 0.5 m/s, 1 m/s, 1.5 m/s and 2 m/s and keeping the load as 70 N and sliding distance as 1000 m constant. Surface of the pin is polished with different grit size emery paper and then washed with acetone to remove the silicon carbide particles which adhere to the surface. The weight of the pin is measured in weighing balance before the test and after the test to find its weight loss. This weight loss reveals the wear behavior of the material used for tribological tests as shown in graphical representation Fig. 10 and Fig. 11.

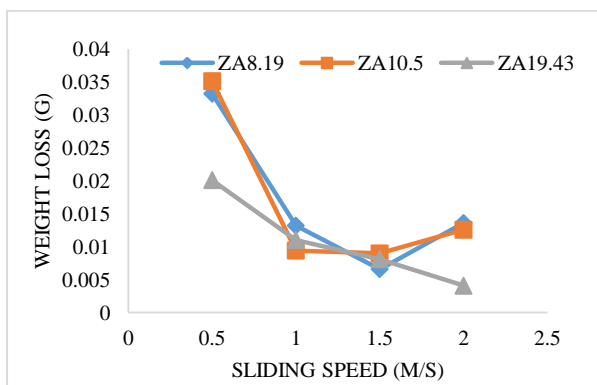


Fig. 10: Weight loss as a function of sliding speed for ZA8.19, ZA10.5 and ZA19.43

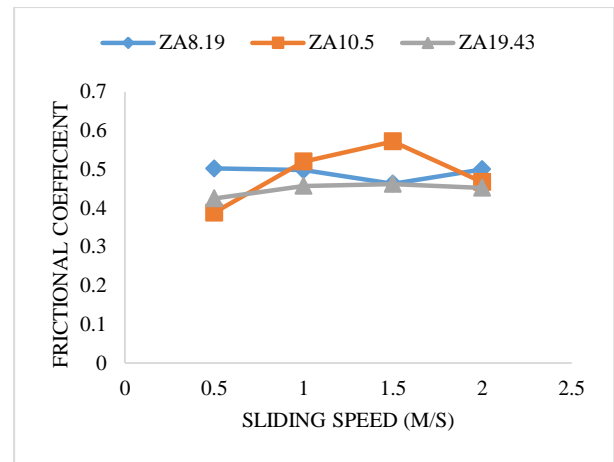
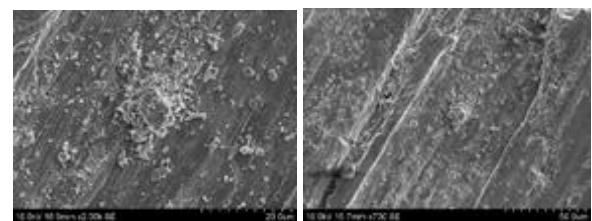


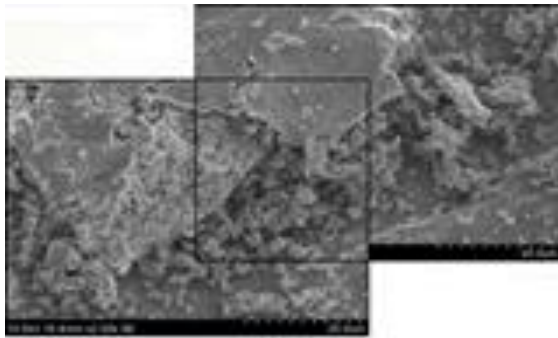
Fig. 11: Frictional coefficient as a function of sliding speed for ZA8.19, ZA10.5 and ZA19.43

Results showed that the weight loss of Zinc-based alloys decreased with increased in sliding speed as seen in Fig. 10. It is known that the leakage of heat from the contact surface is less at high sliding speed, because of which the contact surface temperature is increased. This increases the ability of the sliding surface to interact with the humidity and air. A zinc oxide layer is formed on the contact surface which restrict the two sliding surfaces to have bare contact. Hence, the weight loss is less at higher speed except for the case in which ZA8.19 and ZA10.5 shows a slight increase in weight loss when sliding speed is increased from 1.5 m/s to 2 m/s. At a low sliding speed, the leakage of heat is more, because of which the two sliding surfaces have bare contact. Hence, weight loss is found to be more at low sliding speed. Frictional coefficient of ZA8.19 and ZA19.43 is found to be approximately constant as seen in Fig. 11 and for ZA10.5, it increases with the decrease in weight loss and further decreases beyond 1.5 m/s Sliding speed.



(a) (b)

Fig. 12: Scanning Electron Microscope (SEM) image of ZA10.5 at load 70 N and Sliding speed 1.5 m/s (a) shows smoother surface having loose wear particle which was back transferred during sliding and (b) shows grooves and cracks



(a)



(b)

Fig. 13: Scanning Electron Microscope (SEM) image of ZA10.5 at load 70 N and Sliding speed 2 m/s
(a) shows rough surface and (b) shows grooves and scratches

Fig. 12 (a) showed a smoother surface having loose wear particle which was back transferred during sliding. Grooves and cracks can also be seen in Fig. 12 (b). In Fig. 10, the weight loss of ZA8.19 and ZA10.5 is observed to have slightly increased value when the sliding speed is increased beyond 1.5 m/s. Zinc-Aluminium alloys contains two solid phases mainly α and η . Here α is aluminium rich phase which if added in a definite quantity to Zinc-Aluminium alloys will provide thermal stability and strengthening. Since this phase has fcc structure, so during sliding, it improves the load bearing capability of Zinc-Aluminium alloys which in turn helps in attaining better work hardening capability. Hence, the wear behaviour of Zinc-Aluminium alloys improve. On the other hand, η is Zinc rich phase having hcp structure. This η phase is actually a lubricating phase. When there is increase in sliding speed from 1.5 m/s to 2 m/s, the surface temperature was increased which destroyed the lubricating ability of η phase resulting in more plastic deformation. Hence, rough surface is obtained as seen in Fig. 13 (a) and grooves and scratches can be seen in Fig. 13 (b).

Fig. 14 shows SEM image of the wear debris formed during the tribological test. It is observed that the wear debris are particle like structure, which indicates that the wear occurred is a mild wear. Hence, the dry sliding tribological studies of the three Zinc-based alloys, mainly ZA8.19, ZA10.5 and ZA19.43, with varying Al content using pin-on-disc tribometer is conducted successfully. The experiments reveal that ZA19.43 is a more wear resistant material among three.

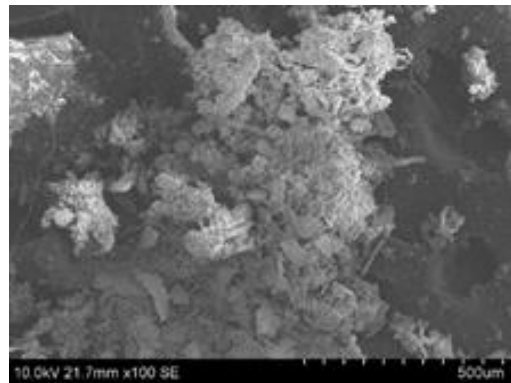


Fig. 14: SEM image of the wear debris formed on the steel disc track

4. CONCLUSIONS

Hardness of Zinc-based alloy increases with the increase in Al-content. Microstructure of ZA8.19 consists of coarse η -Zn rich dendrites and $\alpha+\eta$ eutectoid colonies. Microstructure of ZA10.5 contains finer η -Zn rich dendrites and $\alpha+\eta$ eutectoid colonies more than ZA8.19. Microstructure of ZA19.43 contains α -Al rich dendrites and surrounded by $\alpha+\eta$ eutectoid. In sliding distance test, it is observed that for all cases, the steady-state wear is reached before 1000 m of sliding. Hence, fixing 1000 m as sliding distance is justified. In load test, the weight loss increases with the increase in load except for the case in which beyond 50 N, the weight loss of ZA8.19 decreases as the load is increased. Among zinc alloys, ZA19.43 shows more wear resistance at all loads. Frictional coefficient of ZA19.43 is lower at low loads i.e. 10 N and 30 N. But as the load is increased beyond 30 N, ZA10.5 shows a lower value of frictional coefficient. In sliding speed test, the weight loss decreases with increase in sliding speed except for the case where the weight loss of ZA8.19 and ZA10.5 increases as the speed is increased beyond 1.5 m/s. Frictional coefficients of ZA8.19 and ZA19.43 show approximately constant values with increase in sliding speed. ZA10.5 shows a decrease in weight loss and increase in frictional coefficient as the sliding speed is increased from 0.5 m/s to 1.5 m/s

beyond which the response gets reversed. Overall ZA19.43 is found to be the most wear resistant material among the three.

REFERENCES

- [1] Seenappa, *Tribological studies on Zinc-Aluminium cast alloys*, doctoral diss., Bangalore University, Bangalore, 2016.
- [2] W. Mihaichuk, Zinc Alloy Bearings Challenge the Bronzes, *Machine Design*, 53, 1981, 133-137.
- [3] E. Gervais, H. Levert, and M. Bess, The development of a family of zinc-based foundry alloys, *Transactions of the American Foundrymen's Society*, 68, 1980, 183-194.
- [4] B. K. Prasad, A. K. Patwardhan, and A. H. Yegneswaran, Influence of aluminium content on the physical, mechanical and sliding wear properties of zinc-based alloys, *Zeitschrift fuer Metallkunde/Materials Research and Advanced Techniques*, 88(4), 1997, 333-338.
- [5] M. T. Abou El-khair, A. Daoud, and A. Ismail, Effect of different Al contents on the microstructure, tensile and wear properties of Zn-based alloy, *Material Letters*, 58, 2004, 1754-1760.
- [6] G. L. Kehl, *The Principles of Metallographic Laboratory Practice*, McGraw-Hill, New York, (NY), 1949.
- [7] H. Yalong, *Superhard Materials Co. Ltd.*, available at: <http://m.yalongdiamond.com/en-US/products/grinding-paste.html>, 2017.
- [8] G. V. Voort, *Metallography Principles and Practice*, McGraw-Hill, New York, (NY), 1984.
- [9] H. Elzanaty, Al-addition influence on tribological properties of Zn- based alloys, *International Journal of Research in Engineering & Technology*, 2, 2014, 63-68.
- [10] E. Rabinowicz, *Friction and Wear of Materials*, Wiley, New York, (NY), 1995.
- [11] H. Hirani, *Fundamentals of Engineering Tribology*, Cambridge University Press, India, 2016.